Scaling up the predator functional response in heterogeneous environment: When Holling type III can emerge?

Flora Cordoleani [a,b,*], David Nerini [a], Andrey Morozov [c],
Mathias Gauduchon [a], Jean-Christophe Poggiale [a]

[a] Aix-Marseille Université, Université du Sud Toulon-Var, CNRS/INSU, IRD, MIO, UM 110, 13288 Marseille, Cedex 09, France
[b] Department of Wildlife, Fish, and Conservation Biology, University of California, Davis, One Shields Ave, Davis, CA 95616
[c] Department of Mathematics, University of Leicester, University Road, Leicester LE1 7RH, United Kingdom

HIGHLIGHTS

- The functional response is modified with density-dependent dispersal of predators.
- Emergence of a Holling type III functional response at global scale.
- Stabilization of the predator–prey model in eutrophic environment.
- Enhancement of the system stability with an increase of the patch number.

ARTICLE INFO

ABSTRACT

Accurate parametrization of functional terms in model equations is of great importance for reproducing the dynamics of real food webs. Constructing models over large spatial and temporal scales using mathematical expressions obtained based on microcosm experiments can be erroneous. Here, using a generic spatial predator–prey model, we show that scaling up the microscale functional response of a predator can result in qualitative alterations of functional response on macroscales. In particular, a global functional response of sigmoid type (Holling type III) can emerge as a result of non-linear averaging of non-sigmoid local responses (Holling type I or II). We demonstrate that alteration between the local and the global response in the model is a result of the interplay between density-dependent dispersal of the predator across the habitat and heterogeneity of the environment. Using the method of aggregation of variables, we analytically derive the mathematical formulation of the global functional response as a function of the total amount of prey in the system, and reveal the key parameters which control the emergence of a Holling type III global response. We argue that this mechanism by which a global Holling type III emerges from a local Holling type II response has not been reported in the literature yet: in particular, Holling type III can emerge in the case of a fixed gradient of resource distribution across the habitat, which would be impossible in priorly suggested mechanisms. As a case study, we consider the interaction between phytoplankton and zooplankton grazers in the water column; and we show that the emergence of a Holling type III global response can allow for the efficient top-down regulation of primary producers and stabilization of planktonic ecosystems under eutrophic conditions.

© 2013 Elsevier Ltd. All rights reserved.

1. Introduction

Construction of advanced models of population dynamics requires accurate parameterization of model functions such as growth rates, predation, closure terms, etc. Traditionally, laboratory experiments play a pivotal role when deciding which concrete mathematical formulation to choose to describe the given species and what should be the realistic range of parameters (Luckinbill, 1974; Costantino et al., 1997; Hansen et al., 1997; Fussmann et al., 2000). A major difficulty arises, however, when one wishes to understand the dynamics of the same species on a scale much larger than those of the initial settings (e.g. community or ecosystem levels). Since local interactions between species are often non-linear, it would be insufficient to construct a macroscale model by simply substituting the effective population sizes into a microscale model: one needs to properly incorporate effects of species aggregation, heterogeneity of the environment, patterns of movement behavior, etc., which cannot be observed in small size

* Corresponding author. Tel.: +33 4 91 82 91 26; fax: +33 4 91 82 96 41.
E-mail addresses: fcordoleani@ucdavis.edu,
flora.cordoleani@univ-amu.fr (F. Cordoleani),
david.nerini@univ-amu.fr (D. Nerini, am379@leicester.ac.uk (A. Morozov),
mathias.gauduchon@univ-amu.fr (M. Gauduchon),
jean-christophe.poggiale@univ-amu.fr (J.-C. Poggiale).

laboratory microscosms and mesocosms (Levin, 1992; Gubbins and Gilligan, 1997; Englund and Leonardsson, 2008; Carlotti and Poggiale, 2010; Arditi and Ginzburg, 2012). Thus, the question of how we should modify the initial microscale models to be able to reproduce interactions on a macroscale level remains in the focus in theoretical ecology (Chesson, 1998; Hastings, 2010).

Interestingly enough, dynamics of complex spatially extended ecosystems can be often understood using simpler (reduced) models operating with some integral characteristics, for instance, the population sizes of species (Morozov and Poggiale, 2012). There exist various methods of reducing spatially explicit models such as the aggregation of variables method, scale transition theory and the modified mean-field approach (Chesson, 1998; Iwasa et al., 1987, 1989; Morale et al., 2005; Auger et al., 2008b; Pascual et al., 2011). In reduced models operating on macroscales the terms standing for predation ought to be substantially modified to include the effect of spatial heterogeneity and dispersal of organisms (Gubbins and Gilligan, 1997; Poggiale, 1998; Auger et al., 2000; Pascual et al., 2011), so when constructing a predator–prey model in terms of global variables, accurately scaling up the predator functional response becomes a key issue (Englund and Leonardsson, 2008). It has been shown that scaling up the functional response can result not only in quantitative changes but also in qualitative changes including alteration of the Holling type (Michalski et al., 1997; Poggiale, 1998; Morozov and Arashkevich, 2008; Morozov, 2010). It is not surprising that such an alteration of the functional response can completely modify the key properties of the resultant ecosystem models, such as stability and species persistence (Poggiale, 1998).

In this paper, we extend previous studies on scaling up the functional response of predators in a spatially heterogeneous environment. In particular, we investigate the conditions for the emergence of a global functional response of a sigmoid type (Holling type III) as a result of the non-linear averaging of a non-sigmoid (Holling type II) local response. We suggest a novel mechanism for the emergence of a Holling type III global response which can be observed even for a constant gradient of resource distribution across the system—this differs from previous works in which the emergence of a sigmoidal response required a self-adjusted dynamical gradient of resource distribution. Mathematically, we consider a generic predator–prey model in a patchy environment connected by migration, where the local functional response is assumed to be non-sigmoid. Using the method of aggregation of variables we analytically derive the expression for the predator functional response on the macroscale, and demonstrate that for small prey densities, the clearance rate is an increasing function of the total amount of prey, clearly indicating a type III response. We then show that stabilization of the predator–prey interactions in the model is possible for large values of the prey carrying capacity, which would be impossible at the local scale with a non-sigmoid response.

As a case study, we investigate the interaction between phytoplankton and zooplankton grazers in the water column, which can be considered as a chain of patches connected by turbulent vertical diffusion and active migration of foragers. In many planktonic ecosystems, successful grazing control of phytoplankton growth by herbivores is possible despite a high nutrient supply in the water (Cullen et al., 1992; Armstrong, 1994). However, a large body of experimental work shows that the grazing of zooplankton herbivores is better described by a Holling type I or II (DeMott, 1982; Hirst and Bunker, 2003; Jeschke et al., 2004). Thus, when we implement laboratory-based parameterizations of the functional response in food-web macroscale models with eutrophication, the grazers would not be able to control the population of the prey/primary producers (Oaten and Murdoch, 1975; Scheffer and de Boer, 1995; Fussmann and Blasius, 2005). The results of this paper show that the global functional response of zooplankton herbivores in the whole water column can be of Holling type III, which will provide an extra degree

of stability in models and may explain the control of some plankton bloom initiation in eutrophic waters.

The paper is organized as follows. In Section 2 we introduce the general modeling framework of predator–prey interactions in a patchy environment, describe the local predator–prey interactions and the migration patterns between patches. In Section 3, using the aggregation of variables method we derive the expression for the global functional response and show the emergence of a Holling type III global response, then considering the predator–prey model on macroscale we show stabilization of the system which would be impossible on the local scale (microscale). In Section 4, we compare the mechanism by which the predator functional response is altered and the ecosystem stabilized to those mechanisms reported in earlier works, and we conclude by discussing the limitations of our study.

2. General modeling framework

2.1. The predator–prey model in a patchy environment

We consider predator–prey interactions in a patchy environment, where patches are connected via continuous migration of species. We denote by $x_i(\tau)$ and $y_i(\tau)$ the density of prey and predator respectively in patch i at time τ; thus, the vectors $\mathbf{x}(\tau)$ and $\mathbf{y}(\tau)$ represent the partitioning of species among the patches. The model equations read as follows:

$$\frac{d\mathbf{x}}{d\tau} = M_x\mathbf{x} + \varepsilon\mathbf{F}(\mathbf{x}, \mathbf{y}) \tag{1a}$$

$$\frac{d\mathbf{y}}{d\tau} = M_y(\mathbf{x})\mathbf{y} + \varepsilon\mathbf{H}(\mathbf{x}, \mathbf{y}) \tag{1b}$$

where the functions $\mathbf{F}(\mathbf{x}, \mathbf{y})$ and $\mathbf{H}(\mathbf{x}, \mathbf{y})$ describe growth and predation processes and M_x and M_y are the migration matrices, for prey and predator respectively; the elements d_{ij} and d'_{ij} of the matrices M_x and M_y respectively are the *per capita* migration rate from patch j to patch i. The dimensionless coefficient $\varepsilon \ll 1$ is introduced to take into account the slow scale of population dynamics compared to the fast migration scale, thus ε can be interpreted as the time scaling parameter. We consider the following parameterizations for the functions F_i and H_i:

$$F_i = F_i(x_i, y_i) = r_i x_i\left(1 - \frac{x_i}{k_i}\right) - \frac{ax_i}{b + x_i}y_i,$$

$$H_i = H_i(x_i, y_i) = \frac{eax_i}{b + x_i}y_i - \mu_i y_i.$$

In each patch, the growth of the prey population is described by a standard logistic function, the parameters r_i and k_i being the intrinsic growth rate and the carrying capacity respectively. The local predation is described using a hyperbolic function, the disc-equation (Holling, 1959), which is of type II. The predators increase their biomass by consuming prey, with a conversion factor e, and die naturally at a constant rate μ_i.

2.2. Application of the aggregation of variables method

In the case, where migration of species between patches is a fast process compared to the population dynamics ($\varepsilon \ll 1$), we can reduce the initial model (1) using the aggregation of variables method. The method of aggregation of variables has been widely used in population and community dynamics (see Auger et al., 2008a,b, 2012 for a review of developments and applications). Let us for the sake of simplicity consider that the patches form a chain in space; this can model a sequence of horizontal layers along the vertical water column in planktonic ecosystems. Thus, for each patch individuals of both species are allowed to migrate to the neighboring patches only. We should emphasize that the method can also be applied to the more general situation where patches are connected by long-jump dispersal.

Moreover, we assume that the prey migration rates are constant (density-independent migration) while the predator migration rates are prey dependent. The mathematical parameterization of the predator migration rates will be provided in Section 2.3.

The migration matrices for prey and predator become respectively

$$
M_x = \begin{pmatrix}
-d_{21} & d_{12} & 0 & \dots & & \dots & 0 \\
d_{21} & -d_{12}-d_{32} & d_{23} & \ddots & & & \vdots \\
0 & \ddots & \ddots & \ddots & & & \vdots \\
\vdots & \ddots & \ddots & \ddots & & \ddots & 0 \\
\vdots & & & \ddots & d_{n_{-1}n_{-2}} & -d_{n_{-2}n_{-1}}-d_{nn_{-1}} & d_{n_{-1}n} \\
0 & \dots & & \dots & 0 & d_{nn_{-1}} & -d_{n_{-1}n}
\end{pmatrix},
$$

and

$$
M_y = \begin{pmatrix}
-d'_{21} & d'_{12} & 0 & \dots & & \dots & 0 \\
d'_{21} & -d'_{12}-d'_{32} & d'_{23} & \ddots & & & \vdots \\
0 & \ddots & \ddots & \ddots & & & \vdots \\
\vdots & \ddots & \ddots & \ddots & & \ddots & 0 \\
\vdots & & & \ddots & d'_{n_{-1}n_{-2}} & -d'_{n_{-2}n_{-1}}-d'_{nn_{-1}} & d'_{n_{-1}n} \\
0 & \dots & & \dots & 0 & d'_{nn_{-1}} & -d'_{n_{-1}n}
\end{pmatrix},
$$

where d_{ij} are constant and $d'_{ij} = d'_{ij}(x_j)$ are functions of the local prey density.

Let us denote by x and y the total amount of preys and predators in the system: $x = \sum_{i=1}^{n} x_i$ and $y = \sum_{i=1}^{n} y_i$. In order to apply the aggregation method, let us introduce the frequencies of prey and predator defined by $u_i = x_i/x$ and $v_i = y_i/y$ respectively; these numbers represent the proportion of species in each patch. We obtain the following slow-fast system:

$$
\begin{cases}
\dfrac{du_i}{d\tau} = \sum_{\substack{j=i-1 \\ j>0,\ j\neq i}}^{i+1} d_{ij}u_j - \sum_{\substack{j=i-1 \\ j>0,\ j\neq i}}^{i+1} d_{ji}u_i + \varepsilon F_i(u_i, v_i, x, y) \\
\qquad - u_i \varepsilon \left[\sum_{j=1}^{n} F_j(u_j, v_j, x, y) \right], \quad i = 1, \dots, n-1, \\[2mm]
\dfrac{dv_i}{d\tau} = \sum_{\substack{j=i-1 \\ j>0,\ j\neq i}}^{i+1} d'_{ij}v_j - \sum_{\substack{j=i-1 \\ j>0,\ j\neq i}}^{i+1} d'_{ji}v_i + \varepsilon H_i(u_i, v_i, x, y) \\
\qquad - v_i \varepsilon \left[\sum_{j=1}^{n} H_j(u_j, v_j, x, y) \right], \quad i = 1, \dots, n-1, \\[2mm]
\dfrac{dx}{d\tau} = \varepsilon \left[\sum_{i=1}^{n} F_i(u_i, v_i, x, y) \right], \\[2mm]
\dfrac{dy}{d\tau} = \varepsilon \left[\sum_{i=1}^{n} H_i(u_i, v_i, x, y) \right].
\end{cases}
\tag{2}
$$

The method consists first in setting $\varepsilon = 0$ in (2) and computing the equilibrium of the remaining system written in terms of the state variables $(u_1, \dots, u_{n-1}, v_1, \dots, v_{n-1}, x, y)$. For $\varepsilon = 0$, the global variables x and y are constant and the fast variables u_i and v_i reach a steady state u_i^* and $v_i^*(x)$. Note that the frequencies of the predator population at equilibrium depend on x because the migration matrix of the predator depends on the prey densities on the different patches. Since it can be shown that the fast steady state $(u_i^*, v_i^*(x))$ is always asymptotically stable in our model, the second step of the method consists in replacing the fast variables u_i and v_i by their equilibrium values in the equations of the global (slow) state variables x and y. Using the fact that $x_i = u_i x$ and $y_i = v_i y$ the global-scale system reads

$$
\begin{cases}
\dfrac{dx}{d\tau} = \varepsilon \left[\sum_{i=1}^{n} r_i u_i^* x \left(1 - \dfrac{u_i^* x}{k_i} \right) - \dfrac{a u_i^* x}{b + u_i^* x} v_i^*(x) y \right], \\[3mm]
\dfrac{dy}{d\tau} = \varepsilon \left[\sum_{i=1}^{n} \dfrac{e a u_i^* x}{b + u_i^* x} v_i^*(x) y - \mu_i v_i^*(x) y \right],
\end{cases}
$$

We then get the following reduced (or aggregated) model:

$$
\begin{cases}
\dfrac{dx}{dt} = rx\left(1 - \dfrac{x}{K}\right) - G(x)y + O(\varepsilon), \\[3mm]
\dfrac{dy}{dt} = eG(x)y - \mu y + O(\varepsilon),
\end{cases}
\tag{3}
$$

where $t = \varepsilon\tau$ and the global parameters r, K and μ that respectively represent the global intrinsic growth rate, the global carrying capacity and the global natural predator mortality are functions of the local parameters

$$
r = \sum_{i=1}^{n} u_i^* r_i,
$$

$$
K = \dfrac{r}{\sum_{i=1}^{n} \dfrac{r_i u_i^{*2}}{k_i}},
$$

$$
\mu = \sum_{i=1}^{n} v_i(x)^* \mu_i.
$$

Finally, the general expression of the global-scale functional response, considering a density-dependent predator migration reads

$$
G(x) = \sum_{i=1}^{n} g(u_i^* x) v_i^*(x).
$$

The global functional response is thus given by the sum of all the local functional responses multiplied by the proportion of predators in each patch at the equilibrium. Since we consider that the predation process in each patch is represented by a type II functional response, we obtain the following global functional response expression:

$$
G(x) = \sum_{i=1}^{n} \dfrac{a_i u_i^* x}{b_i + u_i^* x} v_i^*(x),
\tag{4}
$$

where u_i^* and $v_i^*(x)$ are the proportions of prey and predator populations in patch i at the fast equilibrium. In the case we are able to compute the values of u_i^* and $v_i^*(x)$ we can derive the analytical expression for the functional response $G(x)$ and follow possible alteration of Holling type.

2.3. Parameterizing the density-dependent predator migration

To proceed further with analytical derivation of the global functional response $G(x)$ we need to provide a specific mathematical expression for the migration rates of predators (recall that we consider the prey migration to be density independent). Since active dispersal is often energetically costly for animals, we assume that in the case where the resource level in the patch is high it would be preferable to avoid leaving this patch, whereas when the resource is locally scarce it would be beneficial to leave the given patch and start searching in other patches. Therefore, we consider that the rate at which the predator leaves a given patch is a decreasing function of local prey biomass. In the case that the food density in the patch is low, the predator leaves the patch at a constant rate. The simplest possible parametrization of this scenario is the following (cf. Ives, 1992):

$$
d'_{ij}(x_j) = \dfrac{1}{\alpha_{ij} x_j + \gamma_{ij}},
$$

where positive parameters α_{ij} determine the strength of the prey-dependent component of the migration term. The parameters γ_{ij} describe the prey-independent component of migration due to random displacement between the patches.

In the aggregated model, we replace x_j by $u_j^* x$, then the predator displacement rates become

$$d'_{ij} = \frac{1}{\alpha_{ij} u_j^* x + \gamma_{ij}}$$

Finally, we consider that the habitat is heterogeneous, in particular, some patches are safer for the predator than the others. Thus in the case the food is scarce in the system, the predators will migrate towards less dangerous parts of the habitat. For instance, since near the surface the risk of zooplankton consumption by visual predators (e.g. fish) is larger compared to the deep and dark layers, zooplankton grazers should stay in the deepest patches during periods of low phytoplankton levels in the system (Bollens and Frost, 1989; Ohman, 1990; Lampert, 1992). This signifies that in the model we have the following hierarchy $\gamma_{i,i+1} > \gamma_{i,i-1}$ for the coefficients describing the prey-independent (random) component of migration of predators. We consider that the safest patch is patch n, corresponding to the deepest and darkest layer of the water column.

3. Results

In this section we show the emergence of a Holling type III or sigmoid functional response in the predator–prey system at the global scale as a result of non-linear averaging of the Holling type II local responses. This emergence leads to the stabilization of the system dynamics in eutrophic conditions, which would be impossible with a type II predation function.

### 3.1. Emergence of a Holling type III global functional response

For the sake of simplicity, we consider here a three-patches system; however, in Section 3.3 we shall briefly discuss how our findings will depend on the number of patches. For the three-patches model, the predator migration rates are given by

$$d'_{21} = \frac{1}{\alpha_1 x_1 + \gamma_1} = \frac{1}{\alpha_1 u_1^* x + \gamma_1} \quad d'_{12} = \frac{1}{\alpha_2 x_2 + \gamma_2} = \frac{1}{\alpha_2 u_2^* x + \gamma_2}$$

$$d'_{32} = \frac{1}{\alpha_2 x_2 + \gamma_2} = \frac{1}{\alpha_2 u_2^* x + \gamma_2} \quad d'_{23} = \frac{1}{\alpha_3 x_3 + \gamma_3} = \frac{1}{\alpha_3 u_3^* x + \gamma_3}$$

where $\alpha_1 = \alpha_{21}$, $\alpha_2 = \alpha_{12} = \alpha_{32}$, $\alpha_3 = \alpha_{23}$ and $\gamma_1 = \gamma_{21}$, $\gamma_2 = \gamma_{12} = \gamma_{32}$, $\gamma_3 = \gamma_{23}$ are positive constants, and $\gamma_{23} > \gamma_{21}$. The functions $v_i(x)$, as well as the values of u_i^*, are obtained by using the equations $M_x \mathbf{u} = 0$, $M_y \mathbf{v} = 0$ together with the relations $\sum_{i=1}^{3} u_i^* = 1$ and $\sum_{i=1}^{3} v_i^* = 1$, where $\mathbf{u}$ and $\mathbf{v}$ are the vectors of frequencies.

When we implement expression (4) for the global functional response $G(x)$, we find that the emergence of Holling type III becomes possible: an example of such alteration of the type of response is shown in Fig. 1A, where we plot both the global and local functional responses for the indicated set of parameters. The main difference between types II and III functional responses lies in the shape for low prey densities, and one can see from the graph that for a small amount of prey x in the system, the functional response exhibits a self-accelerating increase (which is faster than linear), indicating a type III response. This can also be understood as the fact that $G''(0) < 0$ for type II functional response, while $G''(0) \geq 0$ for type III. To demonstrate more accurately that we indeed have a sigmoid functional response, we also plotted the clearance rate as a function of food density (see Fig. 1B). The clearance rate g is defined by $G(x) = x g(x)$ (Chow-Fraser and Sprules, 1992), and its behavior can indicate which Holling type response we actually have. In particular, an increase in g for low prey density indicates a Holling type III response, whereas a decrease indicates a Holling type II response (Morozov,
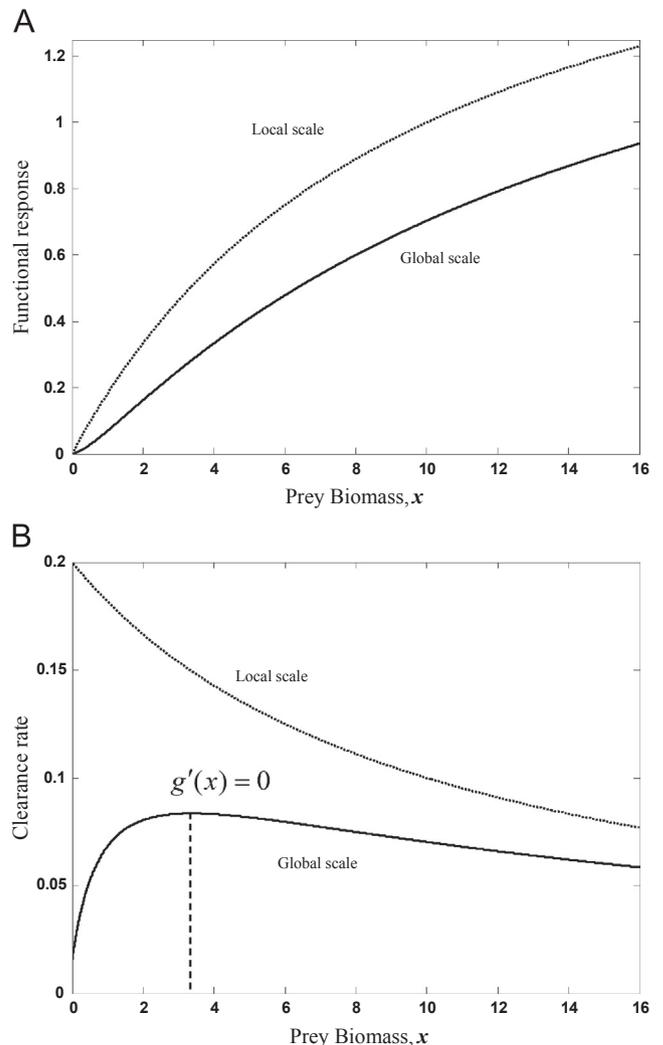
Fig. 1. Alteration of Holling types between the local and the global functional responses in the predator–prey model with fast migration ($\epsilon \ll 1$). (A) The shape of the local and the global functional responses. (B) Clearance rates for the local and the global functional responses. The model parameters are $r_i = 0.8$; $k_i = 500$; $e = 0.5$; $\mu_i = 0.05$; $a = 2$; $b = 10$; $\alpha_1 = 4$; $\alpha_2 = 4$; $\alpha_3 = 4$; $\gamma_1 = 0.5$; $\gamma_2 = 0.5$; $\gamma_3 = 3$; $d_{12} = 0.3$; $d_{21} = 0.1$; $d_{23} = 0.9$; $d_{32} = 0.3$. An increase in clearance rate, for low amount of prey density, indicates a global response of the Holling type III.

2010). From Fig. 1B one can see that for the global response the function $g(x)$ is increasing at small values of x, whereas for the local response $g(x)$ is always decreasing.

To investigate the conditions for which the type of the functional response can be altered, we have derived an analytical expression for $G''(x)$ (see Appendix A) and investigated the sign of $G''(x)$ for small values of x. Note that the condition $G''(x) > 0$ is mathematically equivalent to $g' > 0$ (see proof in Appendix A). We undertook extensive numerical simulations of the analytical expression of $G''(x)$ by varying model parameters, and we found that $G''(0) > 0$ within large range of parameters: in particular, in the case where γ_1 and γ_2 are smaller than γ_3 (Fig. A in Electronic Supplementary Material (ESM) for details). We also proved analytically that for $\gamma_1 \ll \gamma_3$ and $\gamma_2 \ll \gamma_3$ and when the saturation b of the local functional response occurs for a large prey density we always have emergence of a type III functional response (see Appendix A). The latter condition models the biologically meaningful scenario in which the predators tend to move towards deeper layers to avoid their own predators when food in the surface layers is
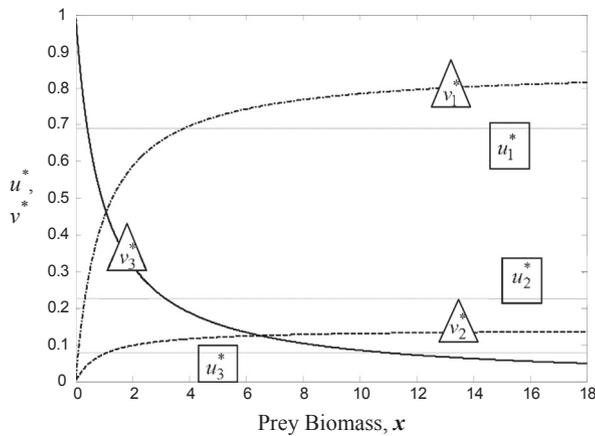
Fig. 2. The evolution of frequencies $u_i^* = x_i/x$ and $v_i^* = y_i/y$ as functions of the total biomass of prey x in the predator–prey model with fast migration ($\epsilon \ll 1$). The model parameters are the same as in Fig. 1. The gradient of the distribution of prey is always constant, whereas the proportion of predators in each patch evolves with the total prey biomass.

scarce. However, in the case that γ_1 becomes greater than γ_3, the value of $G''(0)$ is always negative, which signifies that the global scale functional response remains of type II (see Fig. B in ESM for details). Moreover, the emergence of a sigmoid functional response is impossible in the case that all u_i^* are the same. Thus, spatial heterogeneity due to both the existence of a stable super-critical gradient in the prey distribution across the habitat (i.e. different u_i^*) and unevenness of living conditions for the predator in different patches (different values of $\gamma_{i,i+1}$ and $\gamma_{i,i-1}$), are necessary for the emergence of a type III global response.

Insights into the mechanism of the emergence of a global sigmoid response can be given by looking at Fig. 2, in which we show the evolution of frequencies u_i^* and v_i^* as functions of the total biomass of prey x (which holds on the timescale of population dynamics). At low densities of prey across the patches the predators are mostly localized in patch 3, which is the safest in the habitat. This is a result of the preferential migration of predators towards the safest patch ($n=3$), as described by the model assuming $\gamma_{n-1,n} > \gamma_{i,i-1}$. Since prey migration is fast and performed at a constant rate, the gradient of the distribution of prey is constant (on the timescale of population dynamics), with the density of prey being the lowest in patch n. As a result, most of the predators are exposed to a prey density which is smaller than the average density over the habitat. When the total biomass of prey increases, the food-dependent migration of predators starts playing a role as the predators leave the safest patch n and migrate to other patches, where the food is more abundant (see Fig. 2). This causes a faster than linear increase in the overall intake rate per predator $G(x)$, thus resulting in the emergence of Holling type III global response. At high prey densities in each patch, the effect of saturation starts playing a role and we have a saturated global functional response.

3.2. Stabilization of predator–prey interactions in eutrophic environment

The emergence of a Holling type III response on the global scale translates itself into dumping and suppressing predator–prey oscillations even for large values of the carrying capacity corresponding to a high degree of eutrophication in the system (in particular, in the case the value of K tends to infinity). One can see from Fig. 3A (constructed for the same values of parameters as Fig. 1) that the local densities of prey and predator in each patch tend to a stable equilibrium. Fig. 3B shows the phase plane of the system in terms of the total biomass of species x and y for both the
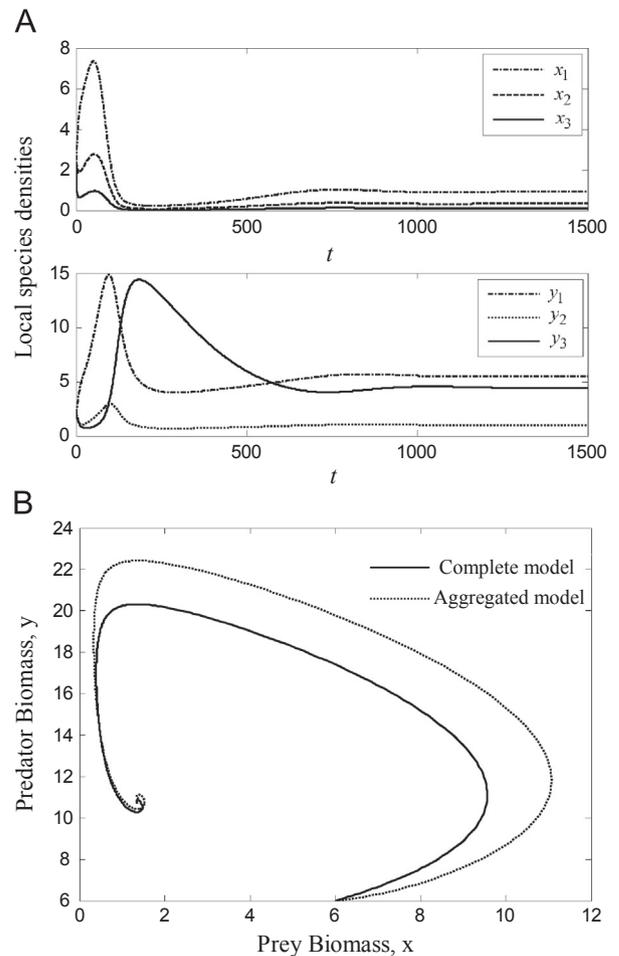
Fig. 3. Stabilization in the predator–prey model with fast migrations ($\epsilon = 0.05$). (A) Temporal dynamics of local species densities in patches. (B) Phase plane of the system showing the dynamics of the total biomass of species x and y for the aggregated and complete models. The carrying capacity of prey in each patch is high ($k_i = 500$) which mimics top-down control in a eutrophic environment. The model parameters are the same as in Fig. 1. The dynamics of prey and predator in each patch as well as the total populations tend to a stable equilibrium on the global scale.

aggregated and complete model ($\epsilon = 0.05$). One can see that for small ϵ the aggregated and complete models show close patterns of dynamics. Note that in the case of fast migration of species one can analytically prove the stabilization in the aggregated model (3), which is actually a standard Rosenzweig–MacArthur model with a Holling Type III functional response (Brauer and Castillo-Chavez, 2000). In Appendix B we show that the fact that the clearance rate g is an increasing function of prey density in the vicinity of the stationary state can guarantee a stable coexistence of prey and its predator for large values of the carrying capacity K. Suppression of oscillations can be possible even for an unlimited carrying capacity of prey, i.e. $K \to \infty$. On the contrary, in the case where the patches are not connected by migration, large values of K would result in system destabilization and high-amplitude oscillations of species densities, finally resulting in extinction of species, which is a well known behavior for a Holling type II functional response (Rosenzweig, 1971).

We should emphasize that the stabilization of the system via predator–prey interactions can only be possible for prey-dependent migration of the predator, and cannot be observed for constant migration rates. This fact can be seen directly from the expression for the global functional response (4). The frequencies of prey and predator $u_i = x_i/x$ and $v_i = y_i/y$ are proportional to the total amount of species x and y, and the global functional response

will be given by a sum of weighted local functional responses, where the weights are constant determined by the predator migration rates. A finite sum of local responses of Holling type II with constant weights will result in a global response of the same type of response (Holling type II) which cannot allow for stabilization (see Appendix B). As such, for large values of the carrying capacity K, persistence in the system becomes impossible since the densities of species through the cycle will regularly take extremely small values. Finally, we should mention that stabilization in the system with large K is possible only in the case where the equilibrium prey density is located in the region where the clearance rate $g(x)$ is increasing, which in the model signifies that the attack rate a and the conversion factor e should be sufficiently large in order to simulate a high predation pressure and reduce the density of prey.

3.3. Impact of the number of patches: a matter of spatial scale

We here briefly address the role of spatial scale and the size of the habitat on the emergence of a global Holling type III functional response in the system and stabilization of the population dynamics. We model expansion in the habitat size by increasing the number of patches n, i.e. adding new patches to the initial chain of patches.

We found that under the same assumptions on the migration rates of prey and predator (see Section 2.3) and considering fast migration rates $\varepsilon \ll 1$, qualitatively similar results would hold as in the case with $n=3$. Namely, the behavior of the clearance rate indicates the emergence of a Holling type III global response ($G''(0) > 0$) and the stabilization of the entire system for large carrying capacities. This fact can be proven analytically in the same way as for $n=3$ but would result in more cumbersome expressions. In Fig. 4A and B we plot the global functional response and the global clearance rate for habitats of different sizes consisting of $n=6$, 8 and 10 patches. We found that by increasing the number of patches (keeping the patch size constant) the global dynamics of the predator–prey system evolves more towards stability. Indeed, the inflection point of the functional response is shifted to higher prey densities when the habitat is expanded by increasing the number of patches. The same holds true for the evolution of the clearance rate slope: the range of prey density where the clearance rate is an increasing function of x becomes wider when n increases, resulting in stabilization of the whole system. Thus, for a large habitat one should expect more efficient top-down control, provided that the assumption of a fast movement of predators and prey across the whole habitat is still satisfied.

4. Discussion and conclusions

In this paper, we emphasize the importance of scaling up the local or microscale predator functional response when modeling food webs on larger spatial scales. We show that a Holling type III functional response can emerge on a global macroscale level from local Holling type II responses, which would have drastic consequences for stability of ecosystems. We also show that increasing the size of the habitat would enhance the emergence of the Holling type III response (see Fig. 4).

Although in earlier theoretical works the possibility of the emergence of a Holling type III on a global scale was demonstrated (Nachman, 2006; Morozov and Arashkevich, 2008; Morozov, 2010), in this paper we suggest a novel ecologically important scenario which has not yet been reported. In particular, the emergence of a Holling type III response in model (1) is possible for constant relative densities of prey across the patches, i.e. for constant frequencies $u_i = x_i/x$, whereas in Morozov and Arashkevich (2008), Morozov
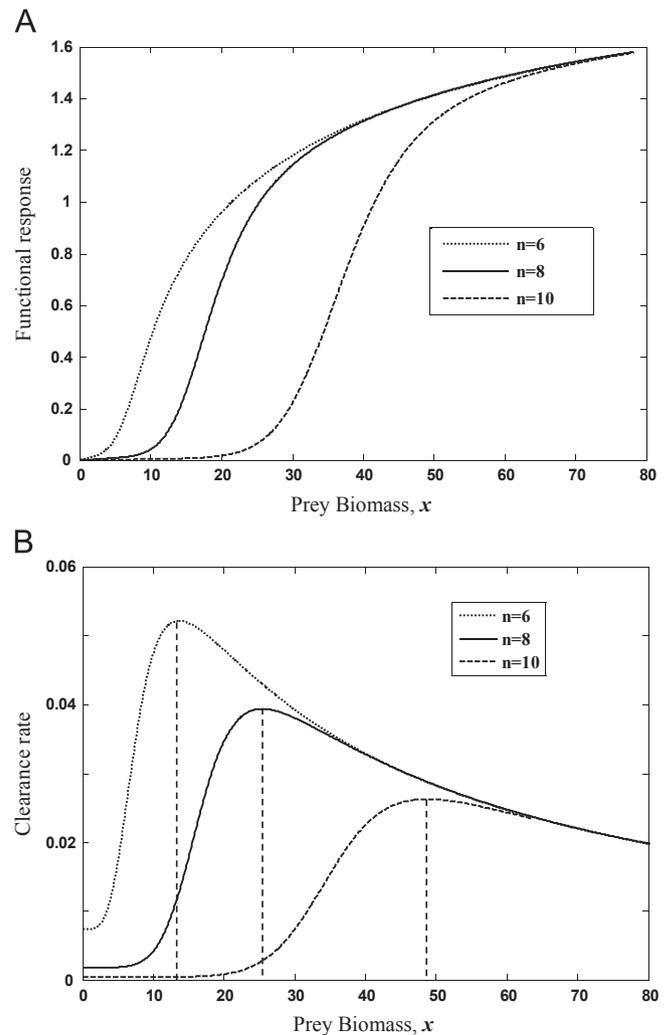
Fig. 4. The global functional response (A) and the clearance rate (B) for the system of $n = 6$, 8 and 10 patches. The model parameters are $a=2$; $b=10$; $\alpha_{12}=\alpha_{nn-1}=4$; $\gamma_{12}=\gamma_{nn-1}=0.5$ and for $i=2,...,n-1$: $\alpha_{ii-1}=4$; $\alpha_{ii+1}=4$; $\gamma_{ii-1}=0.5$; $\gamma_{ii+1}=3$. $d_{12}=d_{65}=d_{87}=d_{109}=0.3$ and for $i=2,...,n-1$: $d_{ii-1}=0.1$; $d_{ii+1}=0.2$. By increasing the number of patches the global dynamics of the predator–prey system evolves towards increased stability.

(2010) the key requirement ensuring the emergence of a type III response of zooplankton grazing on phytoplankton was that the phytoplankton densities should vary with changes in the total amount of phytoplankton x: it was assumed that an increase in x would result in a larger degree of heterogeneity in the phytoplankton distribution across patches, which would eventually cause displacement of zooplankters into patches with higher food abundance and feeding there. In those models an important assumption was made concerning the existence of strong self-shading of phytoplankton in the water column. However, this mechanism might not work in the case of intensive vertical mixing, which would smooth the vertical gradient in the distribution of phytoplankton (Yoshiyama and Nakajima, 2002, 2006). Moreover, a pronounced self shading in the water column is observed mostly for well-developed phytoplankton bloom, and is less pronounced in periods between blooms (Raymont, 1980; Ohman, 1990; Morozov and Arashkevich, 2008). On the other hand, the scenario for the emergence of a type III response suggested in the current paper can cover the above mentioned cases, and explain efficient grazing control in plankton communities with eutrophication.

In model (1) the self-acceleration of the global food intake rate is due to the fact that the spatial distribution of predators follows

the relative abundance of food with an increase of the total amount of food. When the food is scarce the distribution of predators shows more aggregation towards the safest patches, where the proportion of food is the lowest. On the contrary, in Morozov and Arashkevich (2008), Morozov (2010) the spatial distribution of predators was assumed to be homogeneous at low total amount of food, and the self-acceleration of the global food intake rate was due to increasing unevenness in the distribution of predators across patches with an increase of the total amount of food.

The fact that the spatial gradient of prey or resource distribution can be fixed suggests some other real-world case studies where the given mechanism of the emergence of a type III response may be observed. In particular, one can apply the paper findings to those planktonic ecosystems with strong vertical turbulent mixing in the euphotic zone above the thermocline (Deuser, 1987; Venrick, 1993; Law, 2000). In these systems, the distribution of phytoplankton above the thermocline can be close to homogeneous despite pronounced heterogeneity of the light intensity and nutrient concentration (Yoshiyama and Nakajima, 2002, 2006). In this case, patch n corresponding to the lowest density of prey (phytoplankton) will be located below the thermocline, with the other patches being in the upper mixed layer. For instance, if we consider the migration rate of prey $d_{21} = 0.3$ in Fig. 2 and keep the other parameters the same, we obtain $u_1^* \approx u_2^*$, which can mimic homogeneous distribution of phytoplankton above the thermocline.

Our findings can contribute to a resolution of the 'paradox of enrichment' in plankton communities (Rosenzweig, 1971, 1972; Gilpin, 1972; Scheffer and de Boer, 1995; McCauley et al., 1999). This paradox occurs in a generic predator–prey model when an increase in the carrying capacity of the ecosystem results in predator–prey system destabilization; enrichment of the system will lead to cyclic oscillations of large amplitude causing species extinction (Gilpin, 1972; Rosenzweig, 1971; Yodzis and Innes, 1992). However, even if the paradox of enrichment can be obtained in the theoretical models and laboratory experiments (Fussmann et al., 2000), a large number of field data contradict these predictions, suggesting some unknown mechanisms of robust top-down control (Abrams and Walters, 1996; McCauley et al., 1999; Genkai-Kato and Yamamura, 2000). Several mechanisms have been proposed to explain the discrepancy between theory and observation, such as spatial heterogeneity (Jansen, 1995; McLaughlin and Roughgarden, 1991; Petrovskii et al., 2004; Poggiale et al., 2008; Scheffer and de Boer, 1995), an Allee effect in the prey population (Boukal et al., 2007; Kent et al., 2003), a feeding threshold for predators (Bontje et al., 2009) and the introduction of vulnerable and invulnerable classes of prey (Abrams and Walters, 1996). In this paper we show that the paradox of enrichment can be solved simply by increasing the scale of observation: destabilization can indeed be observed on laboratory scales as in Fussmann et al. (2000) but still not observed on global scales.

Finally, we should mention that the mechanism reported here of a Holling type III global response emergence might have its limitations as well. The emergence of a type III response is only possible for systems satisfy several biological assumptions made throughout the study. For instance, the use of the aggregation of variables method needs the identification of two different temporal scales, and we assume here that population dynamics is slow compared to migration process. Moreover, we consider that the predator migration rate depends on prey density in the habitat, but also that when the food is scarce the predator will migrate to the safest patches. We also implicitly make the assumption that the prey spatial distribution in the habitat is heterogeneous. This type of scenario is often observed in planktonic ecosystems, which

thus constitute a perfect case study for the model developed in this paper. The results obtained can still be potentially applied to other ecosystems provided all the above assumptions are satisfied. However, for instance, this model could potentially apply to ecosystems, where predators are highly mobile and have a refuge from top predators, where the food in the refuge is scarce.

Finally, we should point out that at very high levels of food availability there will be sufficient food in the safer patches that the predator can be expected to move there to avoid high predation (Pearre, 1979; Dini and Carpenter, 1992; Dagg et al., 1997), and the parametrization of the prey-dependent migration rate of predator that we consider here becomes invalid in this case. For the global functional response this would signify a decrease of $G(x)$ at large values of x: as a result we should expect to have a Holling type IV response (Andrews, 1968). We are planning to extend the current work to include more realistic patterns of predator migration.

Appendix A. Calculus of the second derivative of the global functional response

Using the analytical expression for $G(x)$ we can find the sign of $G''(0)$, and thus determine the type of the global functional response. The general expression of the global functional response, estimated from the aggregation of variables method, and considering a density-dependent predator migration reads

$$G(x) = \sum_{i=1}^{n} g(u_i^* x) v_i^*(x).$$

Its first derivative is equal to

$$G'(x) = \sum_{i=1}^{n} u_i^* g'(u_i^* x) v_i^*(x) + g_i(u_i^* x) v_i'^*(x).$$

By differentiating a second time, we get the following second derivative:

$$G''(x) = \sum_{i=1}^{n} u_i^{*2} g''(u_i^* x) v_i^*(x) + u_i^* g'_i(u_i^* x) v_i'^*(x) + u_i^* g'_i(u_i^* x) v_i'^*(x)$$
$$+ g_i(u_i^* x) v_i''^*(x)$$
$$= g''(u_i^* x) u_i^{*2} v_i^*(x) + 2 u_i^* g'_i(u_i^* x) v_i'^*(x) + g_i(u_i^* x) v_i''^*(x).$$

In the case of a three-patches predator–prey model and $x=0$, the second derivative reads

$$G''(0) = \sum_{i=1}^{3} [g''_i(0) u_i^{*2} v_i^*(0) + 2 u_i^* g'_i(0) v_i'^*(0)].$$

Since we have considered that the local functional response is type II we have

$$g(x_i) = \frac{a x_i}{b + x_i},$$

$$g'(x_i) = \frac{ab}{(b + x_i)^2}, \quad g'(0) = \frac{a}{b} > 0,$$

$$g''(x_i) = \frac{ab}{(b + x_i)^2}, \quad g''(0) = -\frac{2a}{b^2} < 0.$$

The second derivative of the global functional response for $x=0$ reads now

$$G''(0) = -\frac{2a}{b^2} \left[u_1^{*2} v_1(0) + u_2^{*2} v_2^*(0) + u_3^{*2} v_3^*(0) \right]$$
$$+ \frac{2a}{b} \left[u_1^* v_1'^*(0) + u_2^* v_2'^*(0) + u_3^* v_3'^*(0) \right]. \tag{A.1}$$

The frequencies of species densities in the third patch can be expressed as

$$u_3^* = 1 - u_1^* - u_2^*,$$
$$v_3^*(x) = 1 - v_1^*(x) - v_2^*(x),$$

and thus

$$v_3'^*(x) = -v_1'^*(x) - v_2'^*(x),$$

the expression (A.1) can be rewritten

$$G''(0) = \frac{2a}{b} \left[v_1'^*(0)(2u_1^* + u_2^* - 1) + v_2'^*(0)(2u_2^* + u_1^* - 1) \right]$$
$$- \frac{2a}{b^2} \left[u_1^{*2} v_1'^*(0) + u_2^{*2} v_2'^*(0) + (1 - u_1^* - u_2^*)^2 (1 - v_1'^*(0) - v_2'^*(0)) \right].$$
(A.2)

The values of $v_1^*(x)$ and $v_2^*(x)$ used in the example of the paper read

$$v_1^*(x) = \frac{\alpha_1 u_1^* x + \gamma_1}{\alpha u_1^* x + \gamma_1 + \alpha_2 u_2^* x + \gamma_2 + \alpha_3 u_3^* x + \gamma_3}, \quad v_1^*(0) = \frac{\gamma_1}{\gamma_1 + \gamma_2 + \gamma_3},$$

$$v_2^*(x) = \frac{\alpha_2 u_2^* x + \gamma_2}{\alpha u_1^* x + \gamma_1 + \alpha_2 u_2^* x + \gamma_2 + \alpha_3 u_3^* x + \gamma_3}, \quad v_2^*(0) = \frac{\gamma_2}{\gamma_1 + \gamma_2 + \gamma_3},$$

with the first derivatives

$$v_1'^*(x) = \frac{\alpha_1 u_1^*(\gamma_2 + \gamma_3) - \gamma_1(\alpha_2 u_2^* + \alpha_3 u_3^*)}{(\alpha_1 u_1^* x + \gamma_1 + \alpha_2 u_2^* x + \gamma_2 + \alpha_3 u_3^* x + \gamma_3)^2},$$

$$v_1'^*(0) = \frac{\alpha_1 u_1^*(\gamma_2 + \gamma_3) - \gamma_1(\alpha_2 u_2^* + \alpha_3 u_3^*)}{(\gamma_1 + \gamma_2 + \gamma_3)^2},$$

$$v_2'^*(x) = \frac{\alpha_2 u_2^*(\gamma_1 + \gamma_3) - \gamma_2(\alpha_1 u_1^* + \alpha_3 u_3^*)}{(\alpha_1 u_1^* x + \gamma_1 + \alpha_2 u_2^* x + \gamma_2 + \alpha_3 u_3^* x + \gamma_3)^2},$$

$$v_2'^*(0) = \frac{\alpha_2 u_2^*(\gamma_1 + \gamma_3) - \gamma_2(\alpha_1 u_1^* + \alpha_3 u_3^*)}{(\gamma_1 + \gamma_2 + \gamma_3)^2}.$$

We finally get the following estimation of the global functional response second-order derivative:

$$G''(0) = \frac{2a}{b(\gamma_1 + \gamma_2 + \gamma_3)} \left[\frac{\alpha_1 u_1^*(\gamma_2 + \gamma_3) - \gamma_1(\alpha_2 u_2^* + \alpha_3(1 - u_1^* - u_2^*))}{\gamma_1 + \gamma_2 + \gamma_3} (2u_1^* + u_2^* - 1) \right.$$
$$+ \frac{\alpha_2 u_2^*(\gamma_1 + \gamma_3) - \gamma_2(\alpha_1 u_1^* + \alpha_3(1 - u_1^* - u_2^*))}{\gamma_1 + \gamma_2 + \gamma_3} (2u_2^* + u_1^* - 1)$$
$$\left. - \frac{u_1^{*2} \gamma_1 + u_2^{*2} \gamma_2 + (1 - u_1^* - u_2^*)^2 \gamma_3}{b} \right].$$
(A.3)

The global functional response is a type III if

$$G''(0) > 0 \Rightarrow \frac{\alpha_1 u_1^*(\gamma_2 + \gamma_3) - \gamma_1(\alpha_2 u_2^* + \alpha_3(1 - u_1^* - u_2^*))}{\gamma_1 + \gamma_2 + \gamma_3} (2u_1^* + u_2^* - 1)$$
$$+ \frac{\alpha_2 u_2^*(\gamma_1 + \gamma_3) - \gamma_2(\alpha_1 u_1^* + \alpha_3(1 - u_1^* - u_2^*))}{\gamma_1 + \gamma_2 + \gamma_3} (2u_2^* + u_1^* - 1)$$
$$> \frac{u_1^{*2} \gamma_1 + u_2^{*2} \gamma_2 + (1 - u_1^* - u_2^*)^2 \gamma_3}{b}.$$
(A.4)

For the particular case when $\gamma_1 \ll \gamma_3$ and $\gamma_2 \ll \gamma_3$, which is coherent with the idea that for low amount of food in surface layers predators tend to move toward deeper layers to avoid their own predators, it is strongly likely that

$$\alpha_1 u_1^*(\gamma_2 + \gamma_3) > \gamma_1(\alpha_2 u_2^* + \alpha_3(1 - u_1^* - u_2^*))$$
$$\Leftrightarrow \alpha_1 u_1^*(\gamma_2 + \gamma_3) - \gamma_1(\alpha_2 u_2^* + \alpha_3(1 - u_1^* - u_2^*)) > 0,$$

$$\alpha_2 u_2^*(\gamma_1 + \gamma_3) > \gamma_2(\alpha_1 u_1^* + \alpha_3(1 - u_1^* - u_2^*))$$
$$\Leftrightarrow \alpha_2 u_2^*(\gamma_1 + \gamma_3) - \gamma_2(\alpha_1 u_1^* + \alpha_3(1 - u_1^* - u_2^*)) > 0,$$

in Eq. (A.3).

In that case, $G''(0) > 0$ for instance if

$$2u_1^* + u_2^* - 1 > 0 \Leftrightarrow u_1^* > u_3^*,$$

$$2u_2^* + u_1^* - 1 > 0 \Leftrightarrow u_2^* > u_3^*,$$

and

$$b > \frac{N}{D},$$

with

$$N = (u_1^{*2} \gamma_1 + u_2^{*2} \gamma_2 + (1 - u_1^* - u_2^*)^2 \gamma_3)(\gamma_1 + \gamma_2 + \gamma_3)$$

and

$$D = [\alpha_1 u_1^*(\gamma_2 + \gamma_3) - \gamma_1(\alpha_2 u_2^* + \alpha_3(1 - u_1^* - u_2^*))](2u_1^* + u_2^* - 1)$$
$$+ [\alpha_2 u_2^*(\gamma_1 + \gamma_3) - \gamma_2(\alpha_1 u_1^* + \alpha_3(1 - u_1^* - u_2^*))](2u_2^* + u_1^* - 1)$$

Therefore, a sufficient condition to get a Holling type III global functional response from local Holling type II responses reads

$$\min(u_1^*; u_2^*) > u_3^* \quad \text{and} \quad b > \frac{N}{D}.$$

Finally, let us consider the functional response $G(x) = g(x)x$, with $g(x)$ the clearance rate. It follows:

$$G'(x) = g'(x)x + g(x),$$

then

$$G''(x) = g''(x)x + 2g'(x),$$

and

$$G''(0) = g'(0).$$

Thus the functional response is concave at the origin if and only if the clearance rate increases at the origin.

Appendix B. Link between the clearance rate slope and the predator–prey model stability

Let us consider the following predator–prey model:

$$\frac{dx}{dt} = x(f(x) - g(x)y),$$
$$\frac{dy}{dt} = (eg(x)x - m)y,$$

where x and y are the prey and predator densities respectively. $f(x)$ is the *per capita* growth rate and $g(x)$ is the clearance rate. The functional response is $G(x) = xg(x)$.

(x_e, y_e) is a positive equilibrium if it satisfies the set of equations

$$f(x) - g(x)y = 0,$$
$$eg(x)x - m = 0.$$

The Jacobian matrix at (x_e, y_e) is

$$J = \begin{pmatrix} f'(x_e) - g'(x_e)y_e & -G(x_e) \\ eG'(x_e)y_e & 0 \end{pmatrix}$$

We assume that the functional response is an increasing function of x thus the determinant of J is positive. The equilibrium (x_e, y_e) is thus stable if and only if the trace of J is negative

$$f'(x_e) - g'(x_e)y_e < 0.$$

Let us assume first that $f(x) = r$ which corresponds to a linear growth rate of the prey population. Then the previous condition is equivalent to $g'(x_e) > 0$. Thus an equilibrium is stable if and only if the clearance rate at equilibrium is increasing.

Now, let us assume that $f(x) = r(1 - (x/K))$, as in the present paper, then the stability condition becomes

$$-\frac{r}{K} - g'(x_e)y_e < 0.$$

$g'(x_e) > 0$ is thus a sufficient condition of stability. However, for large values of carrying capacity K (i.e. $K \to \infty$), this condition of stability becomes the necessary condition as well.

Appendix C. Supplementary data

Supplementary data associated with this article can be found in the online version at http://dx.doi.org.10.1016/j.jtbi.2013.07.011.

References

Abrams, P.A., Walters, C.J., 1996. Invulnerable prey and the paradox of enrichment. Ecology 77, 1125–1133.

Andrews, J.F., 1968. A mathematical model for the continuous culture of micro-organisms utilizing inhibitory substance. Biotechnology and Bioengineering 10, 707–723.

Arditi, R., Ginzburg, L.R., 2012. How Species Interact: Altering the Standard View on Trophic Ecology. Oxford University Press.

Armstrong, R.A., 1994. Grazing limitation and nutrient limitation in marine ecosystems: steady state solutions of an ecosystem model with multiple food chains. Limnology and Oceanography 39, 597–608.

Auger, P., Bravo de la Parra, R.B., Poggiale, J.C., Sanchez, E., Nguyen-Huu, T., 2008a. Aggregation of variables and applications to population dynamics. Structured Population Models in Biology and Epidemiology, Series Lecture Notes in Mathematics, sub. Mathematics and Statistics, vol. 1936, pp. 209–263.

Auger, P., Bravo de laParra, R.B., Poggiale, J.C., Sanz, L., 2008b. Aggregation methods in dynamical systems and applications in population and community dynamics. Physics of Life Reviews 5, 79–105.

Auger, P., Poggiale, J.C., Sanchez, E., 2012. A review on spatial aggregation methods involving several time scales. Ecological Complexity 10, 12–25.

Auger, P., S, C., Viala, M., Poggiale, J.C., 2000. Aggregation and emergence in ecological modelling: integration of ecological levels. Ecological Modelling 127, 11–20.

Bollens, S., Frost, B., 1989. Predator induced diel vertical migration in a marine planktonic copepod. Journal of Plankton Research 11, 1047–1065.

Bontje, D., Kooi, B.W., van Voorn, G.A.K., Kooijman, S.A.L.M., 2009. Feeding threshold for predators stabilises predator–prey systems. Mathematical Modelling of Natural Phenomena 4, 91–108.

Boukal, D.S., Sabelis, M.W., Berec, L., 2007. How predator functional responses and alle effects in prey affect the paradox of enrichment and population collapses. Theoretical Population Biology 72, 136–147.

Brauer, F., Castillo-Chavez, C., 2000. Mathematical Models in Population Biology and Epidemiology. Springer, New-York.

Carlotti, F., Poggiale, J., 2010. Towards methodological approaches to implement the zooplankton component in "end to end" food-webs models. Progress in Oceanography 84, 20–38.

Chesson, P., 1998. Making sense of spatial models in ecology. In: Modeling Spatiotemporal Dynamics in Ecology. New York, Springer, pp. 151–166.

Chow-Fraser, P., Sprules, W.G., 1992. Type-3 functional response in limneticsuspension-feeders, as demonstrated by in situ grazing rates. Hydrobiologia 232, 175–191.

Costantino, R.F., Desharnais, R.A., Cushing, J.M., Dennis, B., 1997. Chaotic dynamics in an insect population. Science 275, 389–391.

Cullen, J.J., Lewis, M.R., Davis, C.O., Barber, R., 1992. Photosynthetic characteristics and estimated growth rates indicate that grazing is the proximate control of primary production in the equatorial pacific. Journal of Geophysical Research 97, 639–654.

Dagg, M.J., Frost, B.W., Newton, J.A., 1997. Vertical migration and feeding behavior of calanus pacificus females during a phytoplankton bloom in dabob bay, US. Limnology and Oceanography 42, 974–980.

DeMott, W.R., 1982. Feeding selectivities and relative ingestion rates of Daphnia and Bosmina. Limnology and Oceanography 27, 518–527.

Deuser, W., 1987. Variability of hydrography and particle flux: transient and long-term relationships. Mitt Geol-Palaeont Inst Univ Hamburg 62, 179–193.

Dini, M.L., Carpenter, S.R., 1992. Fish predator, food availability and dielvertical migration in Daphnia. Journal of Plankton Research 14, 359–377.

Englund, G., Leonardsson, K., 2008. Scaling up the functional response for spatially heterogeneous systems. Ecology Letters 11, 440–449.

Fussmann, G.F., Blasius, B., 2005. Community response to enrichment is highly sensitive to model structure. Biology Letters 1, 9–12.

Fussmann, G.F., Ellner, S.P., Shertzer, K.W., G, H.J.N., 2000. Crossing the hopf bifurcation in a live predator–prey system. Science 290, 1358–1360.

Genkai-Kato, M., Yamamura, N., 2000. Profitability of prey determines the response of population abundances to enrichment. Proceedings of the Royal Society of London. Series B 267, 2397–2401.

Gilpin, M.E., 1972. Enriched predator–prey systems: theoretical stability. Science 177, 902–904.

Gubbins, S., Gilligan, C.A., 1997. A test of heterogeneous mixing as a mechanism for ecological persistence in a disturbed environment. Proceedings of the Royal Society of London. Series B 264, 227–232.

Hansen, P.J., Bjornsen, P.K., Hansen, B.W., 1997. Zooplankton grazing and growth: scaling within the 2–2000 m body size range. Limnology and Oceanography, 687–704.

Hastings, A., 2010. Timescales, dynamics, and ecological understanding. Ecology 91, 3471–3480.

Hirst, A.G., Bunker, A.J., 2003. Growth of marine planktonic copepods: global rates and patterns in relation to chlorophyll a, temperature, and body weight. Limnology and Oceanography 48, 1988–2010.

Holling, C.S., 1959. The components of predation as revealed by a study of small-mammal predation of the European pine sawfly. Canadian Enthomologist 91, 293–320.

Ives, A.R., 1992. Continuous-time models of host-parasitoid interactions. American Naturalist 140, 1–29.

Iwasa, Y., Andreasen, V., Levin, S.A., 1987. Aggregation in model ecosystems I. Perfect aggregation. Ecological Modelling 37, 287–302.

Iwasa, Y., Levin, S.A., Andreasen, V., 1989. Aggregation in model ecosystems II. Approximate aggregation. Mathematical Medicine and Biology 6, 1–23.

Jansen, V.A.A., 1995. Regulation of predator–prey systems through spatial interactions: a possible solution to the paradox of enrichment. Oikos 74, 384–390.

Jeschke, J., Kopp, M., Tollrian, R., 2004. Consumer-food systems: why type i functional responses are exclusive to filter feeders. Biological Reviews 79, 337–349.

Kent, A., Doncaster, C.P., T, S., 2003. Consequences for predators of rescue and allee effects on prey. Ecological Modelling 162, 233–245.

Lampert, W., 1992. Zooplankton vertical migrations: implications for phytoplankton-zooplankton interactions. Archiv für Hydrobiologie-Beiheft Ergebnisse der Limnologi 35, 69–78.

Law, C.S., 2000. A mesoscale phytoplankton bloom in polar southern ocean simulated by iron fertilization. Nature 407, 695–701.

Levin, S.A., 1992. The problem of pattern and scale in ecology. Ecology 73, 1943–1967.

Luckinbill, L., 1974. The effects of space and enrichment on a predator–prey system. Ecology 55, 1142–1147.

McCauley, E., Nisbet, R.M., Murdoch, W.W., De Roos, A.M., Gurney, W.S.C., 1999. Large amplitude cycles of Daphnia and its algal prey in enriched environment. Nature 402, 653–656.

McLaughlin, J.F., Roughgarden, J., 1991. Pattern and stability in predator–prey communities: how diffusion in spatially variable environments affects the lotka-volterra model. Theoretical Population Biology 40, 148–172.

Michalski, J., Poggiale, J.C., Arditi, R., Auger, P., 1997. Macroscopic dynamic effects of migrations in patchy predato-prey systems. Journal of Theoretical Biology 185, 459–474.

Morale, D., Capasso, V., Oelschläger, K., 2005. An interacting particle system modelling aggregation behavior: from individuals to populations. Journal of Mathematical Biology 50, 49–66.

Morozov, A., 2010. Emergence of Holling type iii zooplankton functional response: bringing together field evidence and mathematical modelling. Journal of Theoretical Biology 265, 45–54.

Morozov, A., Arashkevich, E., 2008. Patterns of zooplankton functional response in communities with vertical heterogeneity: a model study. Mathematical Modelling of Natural Phenomena 3, 131–149.

Morozov, A., Poggiale, J., 2012. From spatially explicit ecological models to mean-field dynamics: the state of the art and perspectives. Ecological Complexity 10, 1–11.

Nachman, G., 2006. A functional response model of a predator population foraging in a patchy habitat. Journal of Animal Ecology 75, 948–958.

Oaten, A., Murdoch, W.W., 1975. Functional response and stability in predator–prey systems. The American Naturalist 109, 289–298.

Ohman, M.D., 1990. The demographic benefits of diel vertical migration by zooplankton. Ecological Monographs 60, 257–281.

Pascual, M., Roy, M., Laneri, K., 2011. Simple models for complex systems: exploiting the relation between local and global densities. Theoretical Ecology 4, 211–222.

Pearre, S.J., 1979. Problems of detection and interpretation of vertical migration. Journal of Plankton Research 1, 29–44.

Petrovskii, S., Li, B.-L., Malchow, H., 2004. Transition to spatiotemporal chaos can resolve the paradox of enrichement. Ecological Complexity 1, 37–47.

Poggiale, J.C., 1998. Predator–prey models in heterogeneous environment: emergence of functional response. Mathematical and Computer Modelling 27, 63–71.

Poggiale, J.C., Gauduchon, M., Auger, P., 2008. Enrichment paradox induced by spatial heterogeneity in a phytoplankton–zooplankton system. Mathematical Models of Natural Phenomena 3, 87–102.

Raymont, J.E.G., 1980. Plankton and Productivity in the Oceans. Phtyoplankton. Pergamon, Oxford.

Rosenzweig, M.L., 1971. Paradox of enrichment: destabilization of exploitation ecosystems in ecological time. Science 171, 385–387.

Rosenzweig, M.L., 1972. Enriched predator–prey systems: theoretical stability. Science 177, 902–904.

Scheffer, M., de Boer, R.J., 1995. Implications of spatial heterogeneity for the paradox of enrichment. Ecology 76 (7), 2270–2277.

Venrick, E.L., 1993. Phytoplankton seasonality in the central north Pacific: the endless summer reconsidered. Limnology and Oceanography 38, 1135–1149.

Yodzis, P., Innes, S., 1992. Body size and consumer-resource dynamics. American Naturalist 139, 1151–1175.

Yoshiyama, K., Nakajima, H., 2002. Catastrophic transition in vertical distributions of phytoplankton: alternative equilibria in a water column. Journal of Theoretical Biology 216, 397–408.

Yoshiyama, K., Nakajima, H., 2006. Catastrophic shifts in vertical distributions of phytoplankton. The existence of a bifurcation set. Journal of Mathematical Biology 52, 235–276.